AIAA 80-0326R

Analysis of Strake Vortex Breakdown Characteristics in Relation to Design Features

Neal T. Frink*
North Carolina State University, Raleigh, N. C.
and
John E. Lamar†
NASA Langley Research Center, Hampton, Va.

This paper describes a water-tunnel study of the vortex breakdown characteristics of a large number of analytically designed vortex strakes tested in combination with a moderate-aspect-ratio trapezoidal wing. A wide range of strake sizes and slenderness ratios are covered, and examples of the effects of the primary design parameters of size, span, and slenderness on the vortex breakdown characteristics are presented and analyzed in relation to the three-dimensional leading-edge suction distributions. Several examples of detailed planform shaping on strakes of the same general size and slenderness are shown. From these it is demonstrated that vortex stability can be improved by satisfying the design criterion. The criterion states that those shapes having leading-edge suction distributions which increase more rapidly near, and have a higher value at, the spanwise tip of the strake promote vortex stability.

Nomenclature

A	= aspect ratio
AD	= analytically designed
b	= span
C	= constant pressure specification
c	= local chord
c_r	= root chord
$(c_r)_w$	= wing root chord, see Fig. 8
c_s	= local suction coefficient
ED	= empirically designed
K_v	= leading-edge vortex lift factor
l	= overall length
P	= polynomial pressure specification
R_a	$= S_s/S_{ref}$
R_b	$= [(b/2)_s/(b/2)_w]_{exp}$
R_s	$= [l/(b/2)]_s$
R.F.	= related flow
r	= radius
S	= area
s	$= (c_s c)/\alpha^2 (b/2)_s$
3-D	= three-dimensional
x	= distance ahead of wing trailing edge at wing-fuselage juncture, see Fig. 8
x'	= distance aft of local leading edge
α	= angle of attack, deg
ΔC_p	= lifting pressure coefficient
η_s	= fractional distance along exposed strake semispan
θ	$= \cos^{-1}(1-2x'/c)$
Λ	= leading-edge sweep angle, positive for sweepback, deg

Subscripts

BD-TE	= strake vortex breakdown at the wing trailing edge
exp	= exposed
ref	= reference
s	= strake
t	= value at the tip
w	= wing
ws	= wing-strake

Presented as Paper 80-0326 at the AIAA 18th Aerospace Sciences Meeting, Pasadena, Calif., Jan. 14-16, 1980; submitted Feb. 11, 1980; revision received June 30, 1980. This paper is declared a work of the U.S. Government and therefore is in the public domain.

*Research Assistant, Mechanical and Aerospace Engineering Department. Member AIAA.

†Aeronautical Research Scientist, STAD. Associate Fellow AIAA.

Introduction

THE strake-wing configurations which are a fundamental design feature of the current lightweight fighters are of continuing interest because of: 1) their ability to generate large amounts of lift during transonic-maneuver conditions, and 2) the achievement of this benefit with low gust response, relatively low structural weight, and relatively small impact on cruise aerodynamics. The first feature results from the ability of the strake to develop vortex lift on itself due to the strong separation-induced vortex flow. This flow (as shown in Fig. 1) also provides a favorable interference lift on the wing through an interaction with the wing flowfield. The second group of features are associated with the low aspect ratio and relatively small size of the strakes.‡ A limit to the maximum lift to be developed by this type of flow does exist, of course, and is reached when the angle of attack is sufficiently high so that large-scale vortex breakdown (described in Ref. 1 as "an abrupt increase in the effective diameter of the rotational core associated with the vortex") occurs over the wing. Therefore, one of the prime considerations in strake design, and the one addressed herein, is the maintenance of a well-organized vortex system over the wing to as high an angle of attack as possible.

During the development of the lightweight fighters, over 100 strakes were tested by each company[2,3] before final selections were made. One reason for the large number of strakes tested was that no parametric strake data base was available. Furthermore, there was no mathematical or empirical design procedure generally available to aid in defining strake shapes which would have a well-organized vortex to high angles of attack or lift coefficients. Since then, a design procedure for a simple strake alone has been developed[4]

‡In particular, at cruise it is possible that the small impact of the strake may be attainable only by the use of camber or dihedral so as to "unload" the strake under this condition. Neither one of these is addressed in this paper, as only planar strakes are considered.

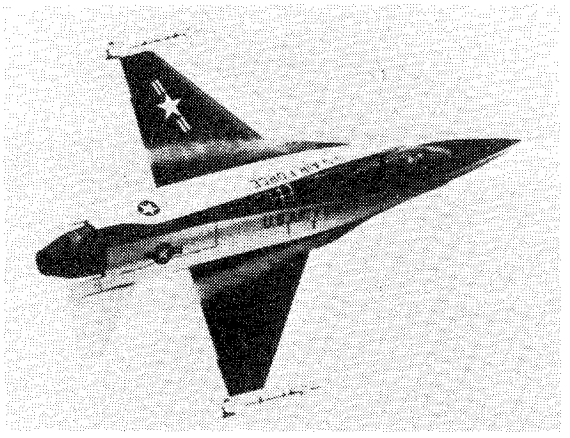

Fig. 1 F-16 strake vortex (from *Aviation Week and Space Technology*).

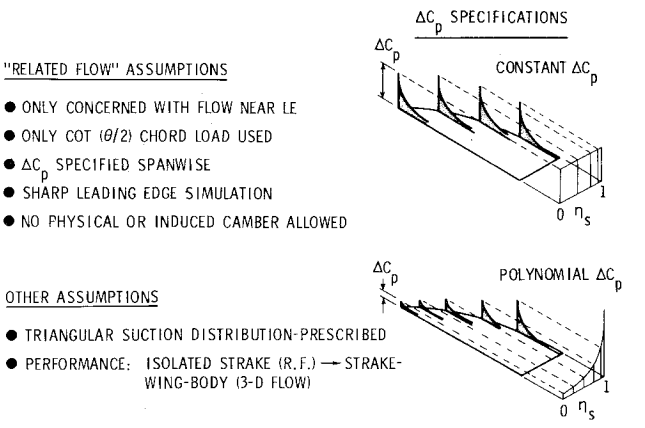

Fig. 2 Features of isolated strake design process.

which relates prescribed leading-edge suction distributions to strake shape through a simplified analytical model. The original application of this procedure, in which a suction that generally increased toward the tip was prescribed, led to the encouraging results reported in Ref. 4. This prompted the use of the procedure to design other strakes of a generic family through which the relationships between strake geometry and the angle of attack for strake-vortex breakdown across the wing trailing edge might be better established. Furthermore, these strakes give an opportunity for additional comparisons between the prescribed and resulting three-dimensional leading-edge suction distributions, the latter including wing-body interactions, to be made and to determine which features are properly represented. Lastly, this generic family will allow an assessment as to whether the design procedure can produce strake shapes that are better than the one originally designed and should provide additional guidance with regard to the suction distribution design criterion.

A water-tunnel test was determined to be an economical way of obtaining the required flow visualization data on a large number of strake-wing-body configurations. Because of their mutual interest, the Northrop Corporation/Aircraft Division agreed to support these tests by building models and providing the water-tunnel facility and operating personnel to assist the authors during the test.

The purpose of this paper is to describe the development of the generic families of strakes and to review selected results from the water-tunnel tests in relation to certain design features.

Strake Design Procedure

Design Criterion

The procedure is based on a design criterion that those strake shapes which, in attached three-dimensional flow, develop more triangular spanwise leading-edge suction distribution§ (peaking near the tip) will provide vortex flow characteristics consistent with a need to delay vortex breakdown to higher angles of attack. (This may be interpreted in a physical sense for separated flows—with the aid of the leading-edge suction analogy—in that they are more stable for shapes which have higher levels of separation induced vorticity near the tip.) This triangular-type suction distribution, along with an appropriate pressure specification and several fixed geometric parameters, is incorporated in the design of an "isolated" strake in a simplified flow. This simplified flow, which is related to three-dimensional potential flow through certain assumptions described below, is useful in the design of a large parametric series of vortex strakes, and can help to isolate the effects of design variables on the resulting geometries.

Assumptions

The assumptions employed in this procedure are listed in Fig. 2 and lead to a flow which is called, for simplicity, the related flow. With respect to three-dimensional potential flow, the related flow has these features:

1) Only flow characteristics near the leading edge are considered because of the interest in leading-edge suction.

2) The only chord loading term ΔC_p used is that for the angle of attack, cot $(\theta/2)$.

3) The chordwise ΔC_p is scaled spanwise in a specified manner, either as a constant or a polynomial (as illustrated in Fig. 2).

4) The constant spanwise specification simulates a sharp leading edge in that, if the pressure is less than a certain local minimum value, the flow will separate at that location and consequently at all others.

5) No physical or induced camber is allowed or simulated in the design.

There are two other assumptions making use of this related flow which are of a more general nature. The first is that the suction distribution across the leading edge can be prescribed and, when used in combination with the ΔC_p specification, almost completely determines the strake shape.[4] The second is that if the strake vortex, which is simulated on the isolated strake in related flow, can be made more stable by using the design criterion, then that strake might also provide a more stable vortex when used in combination with a wing-body configuration in three-dimensional flow. Consequently, comparisons will be made using both suction distributions, although the three-dimensional ones are the more germane with respect to the vortex breakdown data.

A variety of input suction distributions and ΔC_p specifications have been used in the design procedure, and the resulting strake shapes and input variables are given in the next section.

Strake Shapes Studied

Analytically Designed

The 24 strakes employed in the investigation of Ref. 5 were selected from over 200 designed shapes. They were determined by perturbing the prescribed suction distribution used in Ref. 4 in 13 different ways. In order to facilitate strake

§The use of the spanwise distribution of leading-edge suction herein does not imply that the longitudinal variation is unimportant, only that the projection of suction onto the cross-plane provided a more convenient way to approach the problem. It is recognized that certain critical aspects of vortex flow dynamics generally arise from fluid properties along the vortex core, i.e., longitudinal direction.

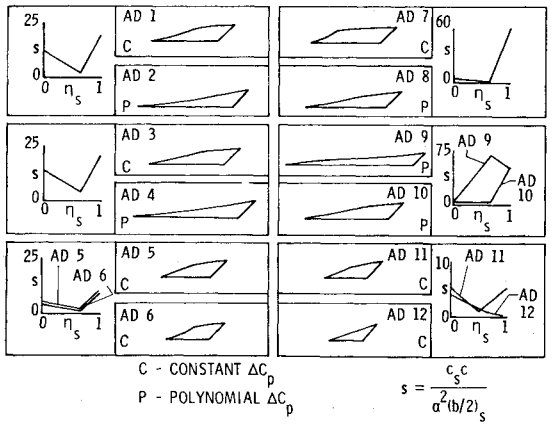

Fig. 3 Analytically designed strakes, reflexive group.

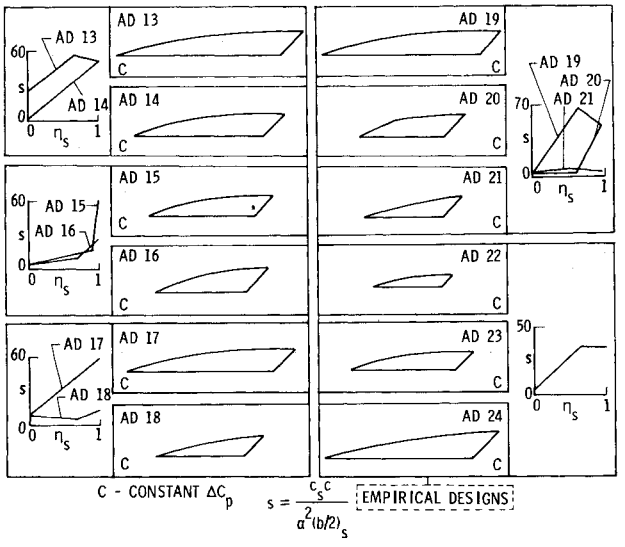

Fig. 4 Analytically designed strakes, gothic group.

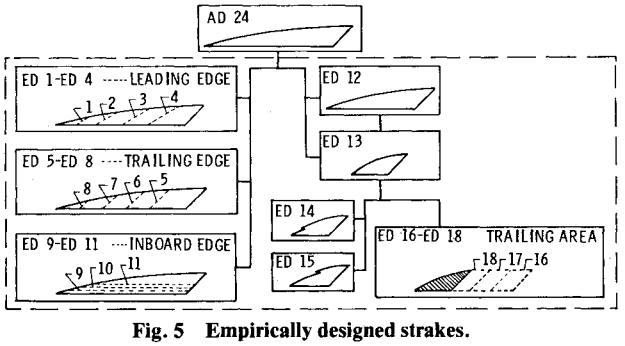

Fig. 5 Empirically designed strakes.

identification, the strakes are characterized according to resulting shapes, reflexive or gothic, and are presented in Figs. 3 and 4 at various scalings. With regard to the reflexive-shaped strakes, 12 were chosen (Fig. 3) as being representative of the group and were tested. For the gothic-shaped strakes, a large number were produced by the method and 12 were chosen (Fig. 4) to provide examples of representative slenderness ratio and initial sweep combinations. Three of the gothic shaped strakes (AD 22-AD 24) have the same shape, but are scaled to different areas. In addition to the strake geometries, Figs. 3 and 4 show the corresponding prescribed leading-edge suction distributions employed in designing the strakes and are characterized by two adjoining line segments of different slope. The specified spanwise pressure

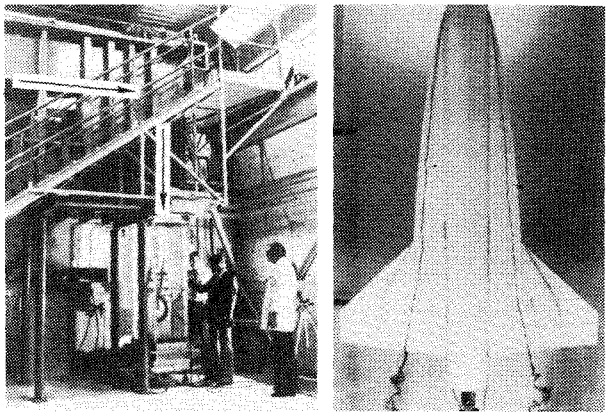

Fig. 6 Northrop diagnostic water tunnel and sample breakdown: left, 16×24 in.; right, AD 24 at $\alpha = 20$ deg.

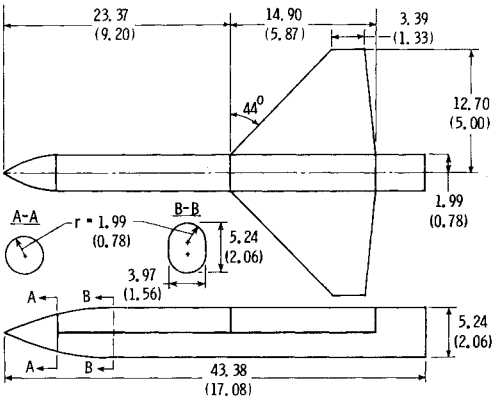

Fig. 7 Water-tunnel wing-fuselage model with wing in forward position (aft wing position is 2.21 cm (0.87 in) rearward).

distributions, which are illustrated in Fig. 2, are designated in these figures by either a *C* or *P* signifying a constant or polynomial ΔC_p distribution, respectively.

Empirically Designed

Several empirical geometric variations were made to the original gothic strake (AD 24) designed in Ref. 4. This group of empirically designed strakes is shown in Fig. 5. Some of the variations (ED 1-ED 13) pertained to techniques for reducing the chord of an existing strake, i.e., scaling down in chord or cutting it off with the intent of achieving a minimum sacrifice of the good performance qualities of the AD 24. Other variations were attempted to improve the vortex breakdown qualities of an already "too short" strake (ED 14-ED 18).

In this paper the strake-wing-body configurations are referred to by the isolated strake designations.

Test Facility and Procedure

The test facility used was the Northrop 16×24 in. Diagnostic Water Tunnel (shown on the left in Fig. 6). It features a closed return with both horizontal and vertical test sections; in the tests described here the downward-flow vertical test section was used. (A model can be seen in this section just to the left of the Northrop personnel.) The test conditions were: velocity ≈0.15 m/s (≈0.5 ft/s), Reynolds number $\approx 1.76 \times 10^4$ based on the mean aerodynamic chord, with α variation of 0-50 deg. Sideslip could also be varied but was set to zero for the results reported herein. While it is recognized that vortex breakdown can have important effects on lateral directional characteristics, the purpose of this initial study was to identify the more promising strakes for further and more complete water-and wind-tunnel testing in which sideslip effects may also be considered.

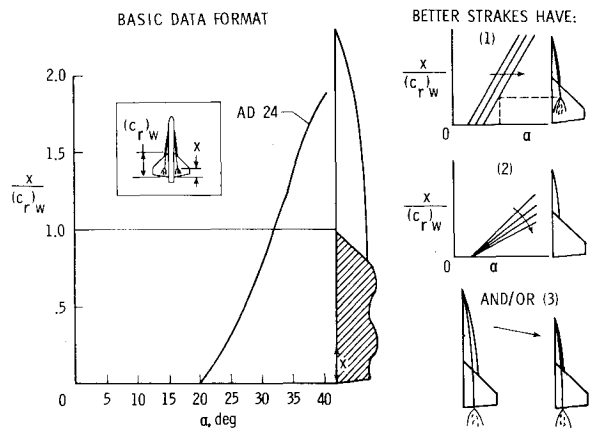

Fig. 8 Sample presentation and interpretation of breakdown data ($R_a = 0.325$).

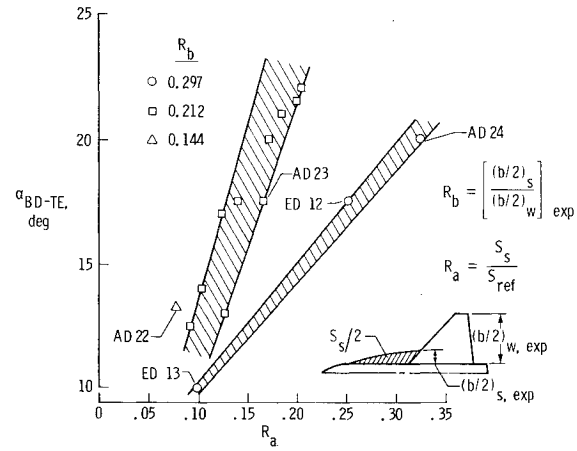

Fig. 9 Effect of R_b on $\alpha_{BD\text{-}TE}$ -R_a relationship (gothic-type strakes).

Table 1 Wing reference quantities

A	2.5	S_{ref}	258 cm^2 (40 in.^{2})
Λ	44 deg	b_{ref}	25.4 cm (10 in.)
c_t/c_r	0.2	c_{ref}	11.66 cm (4.59 in.)

The test procedure was to align the model so that at both high and low α symmetrical strake vortex breakdown patterns were produced. This was accomplished by noting the behavior of the dye injected into the strake vortex core. When the dye became unstable or exhibited reversal of direction, breakdown was said to have occurred. An example of this phenomenon is shown on the right of Fig. 6 for the AD 24 configuration at $\alpha = 20$ deg. Here, breakdown is observed as an instability in the vortex core behind the wing trailing edge. After symmetry was established, the α was increased from 10 deg in 2 deg increments until breakdown occurred near the trailing edge and then in 1 deg increments. After strake vortex breakdown occurs ahead of the wing trailing edge, the α increment is increased once again to 2 deg. Scribed lines on the wing and strake surfaces aided in establishing the vortex breakdown position. The wing used in this test is described in Table 1 and Fig. 7.

Analysis of Results

Data Format and Performance Assessment

A sample of the graphical presentation of the strake vortex breakdown position obtained from the water-tunnel tests is shown in Fig. 8 for the AD 24 strake configuration. By presenting the breakdown data in this manner, the forward progression of breakdown with angle of attack can be easily visualized relative to planform geometry. Since the wing is the main lifting surface, the interaction of the strake vortex flowfield with the wing pressure field is of primary interest. Therefore, the chordwise vortex breakdown position x is nondimensionalized by $(c_r)_w$ to make the results directly comparable over the wing for different strake-wing configurations. Vortex breakdown over the strake is not directly comparable between configurations but its absolute location can be observed relative to the generating strake shown in the center of Fig. 8. The type of line segment used to connect the data points is the same as that used to describe the perimeter of the strake.

The sketches on the right of Fig. 8 illustrate how strake performance is assessed with respect to its vortex breakdown characteristics. Strake performance is based on 1) the angle of attack at which the strake vortex breakdown crosses the wing trailing edge $\alpha_{BD\text{-}TE}$, 2) the rate at which the breakdown progresses forward over the wing once $\alpha_{BD\text{-}TE}$ is reached, and/or 3) the efficiency of strake area. As shown in the upper

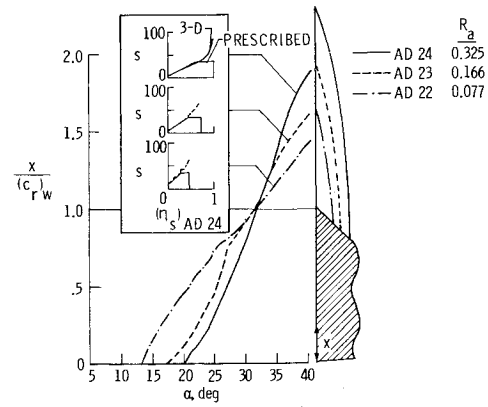

Fig. 10 Effect of strake area on breakdown and suction (fixed-strake shape, $R_s = 7.0$).

sketch, the better strakes are those which have as high an $\alpha_{BD\text{-}TE}$ as possible. This feature is important because the occurrence of vortex breakdown over the wing is realized as a subsequent loss in lift. The middle sketch illustrates that once vortex breakdown crosses the wing trailing edge, it is better to have a low rate of forward breakdown progression with increasing α. This low rate is desirable because a more gradual loss in wing lift promotes milder stall characteristics. The lower sketch illustrates that if the design approach proposed can produce reductions in strake area while maintaining the same angle of attack for vortex breakdown, then a more efficient strake would result.

Effects of Major Geometric Parameters

Though the strake design problem is one of many variables, the major geometric parameters are area, slenderness, semispan, and planform shaping. The effects of these variables as well as their relationships to one another are illustrated by results selected from the gothic-type strakes in the following paragraphs.

Area/Semispan

As pointed out earlier, the design process used to develop the generic families of strakes considered only the isolated strake. However, when these strakes are combined with the wing the ability of the strake vortex to penetrate the wing flowfield is, of course, a strong function of the size of the strake relative to the wing.

Using the results of the gothic-type strakes, Fig. 9 presents the measured angle of attack corresponding to vortex breakdown at the wing trailing edge $\alpha_{BD\text{-}TE}$ as a function of the ratio of exposed strake area to wing reference area, R_a.

Three values of strake semispan are represented and are identified by the cross-hatched bands for two cases and by the single point, AD 22, for the third. The effect of area on $\alpha_{BD\text{-}TE}$ is seen in Fig. 9 to be an expected one of increasing $\alpha_{BD\text{-}TE}$ with increasing R_a. Also from this figure, a further relationship is established for strakes of different semispan. In particular, the data for strakes of $R_b = 0.212$ lie within a band which is above and has a higher slope than a similar band bounding the data for strakes with $R_b = 0.297$. From the two bands the consequence of increasing R_b at a fixed R_a can clearly be seen to reduce the $\alpha_{BD\text{-}TE}$. This can be better understood when it is put in terms of the change in slenderness ratio, i.e., increasing R_b for fixed R_a generally results in a less slender strake. This earlier vortex breakdown associated with reduced slenderness is not surprising since such a trend has been well established for isolated planforms by earlier researchers (e.g., Ref. 1).

With the general trends for both area and slenderness changes in regard to $\alpha_{BD\text{-}TE}$ having been illustrated by Fig. 9, the detailed results of breakdown progression will be illustrated in the next two sections. The first will deal with area scaling and the second with slenderness variations.

Area Scaling

Figure 10 presents the vortex breakdown characteristics as well as the prescribed and three-dimensional suction distributions for the AD 24, AD 23, and AD 22 strakes which are of fixed shape but scaled in size. (The prescribed s-η_s distribution for the AD 23 and AD 22 is identical to that for the AD 24.) Regarding breakdown, the vortex for a smaller strake must persist over a greater relative distance to the wing trailing edge and must penetrate through a stronger adverse wing pressure gradient relative to its vortex strength than that for a larger strake. Hence, it is anticipated that $\alpha_{BD\text{-}TE}$ will decrease as a strake is scaled down in area, which is confirmed by the data.

Another interesting characteristic of these scaled strakes is the manner in which the breakdown data cross $x/(c_r)_w = 1$ at $\alpha \approx 32$ deg. This characteristic is related to the identical but scaled shaping of the strake. It is expected that each of these strakes would have the same vortex breakdown characteristics if tested alone without a wing-body configuration. Hence, it is seen for $\alpha > 32$ deg that even in the presence of a wing-body, the strakes behave somewhat as they would when tested alone, with the differences in breakdown progression being more related to the differences in strake to wing chord. This feature is further evidenced by noting that at $\alpha = 40$ deg the vortex breakdowns occur at approximately one third of $(c_r)_s$ from the apex of each respective strake.

Shown as an insert in Fig. 10 are the leading-edge suction distributions normalized on the AD 24 strake semispan $s-(\eta_s)_{AD\ 24}$ for the strakes in the two assumed flowfields. The two-segmented trapezoidal curve is the prescribed distribution from which the strake was designed. The other curve is the three-dimensional potential flow distribution determined by applying an analysis method to the designed strake in the presence of the wing and body. The latter distribution was calculated by an extended version of the vortex lattice method of Ref. 6. (This version utilized the side-force calculation to extract the leading-edge suction as a means of alleviating a problem associated with the leading-edge thrust computations.) The suction distributions calculated for the complete configurations are, of course, more representative of the actual distributions developed on the strakes and are used as an aid in the analysis.

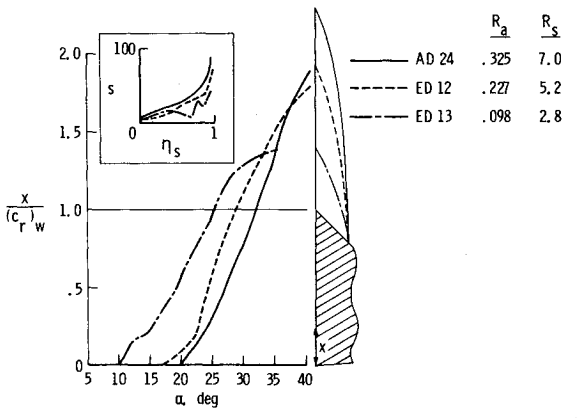

Fig. 11 Effect of strake area/slenderness on breakdown and suction (fixed R_b, gothic strakes).

These three sets of curves show that in addition to the $\alpha_{BD\text{-}TE}$ decreasing with decreasing R_a, the three-dimensional leading-edge suction values at the tip s_t have a similar decrease with strake area. Furthermore, it is seen that the area under the s-$(\eta_s)_{AD\ 24}$ curves (proportional to K_v) decreases with decreasing strake area. Interestingly though, each three-dimensional suction distribution across the inboard spanwise region is in good agreement with its respective prescribed curve. The agreement leads to some understanding of how the design method may be useful as a general guide in generating new strakes; because the vortex stability, as reflected primarily in $\alpha_{BD\text{-}TE}$ and used as a measure of performance, is associated through the design criterion to suction distribution, there is an implication about the correctness of the last design procedure assumption regarding the two flow situations.

Slenderness Variation

In the design of fighter configurations, the strake span may be fixed due to other design constraints. With a fixed strake span, variations in strake area required to generate a desired vortex lift result in variations in slenderness ratio. A parametric series illustrating this condition is shown in Fig. 11 where the vortex breakdown data and corresponding s-η_s curves for three gothic strakes of varying area and slenderness ratio are shown. Once again, $\alpha_{BD\text{-}TE}$ as well as s_t and area under the s-η_s curves decrease with decreasing strake area. However, these decreases may not entirely be attributed to the area effect since R_s is also changing.

To see this better, a performance comparison is made between the ED 13 and AD 22 strakes. Note how the $\alpha_{BD\text{-}TE}$ for the ED 13 strake of Fig. 11 is less than that for the AD 22 strake shown in Fig. 10, although the ED 13 strake has a larger area. Similar results are also seen in the two figures for the ED 12 and AD 23 strakes. Furthermore, α_{BD} decreases at $x/(c_r)_w = 1$ for the three strakes of Fig. 11, whereas breakdown at $x/(c_r)_w = 1$ for the AD 22, AD 23, and AD 24 strakes in Fig. 10 occurred at the same α. Hence, it is shown that slenderness ratio is an important parameter affecting strake performance—the higher being better. This feature is further demonstrated next along with shape effect for strakes of fixed area.

Planform Shaping

In addition to providing a wide range of data related to strake size and slenderness ratio, the study also provides results related to the effects of detailed shaping of the planform. As indicated in Figs. 3 and 4, the designed shapes were based on a variety of prescribed leading-edge suction distributions and, therefore, should provide data to allow at least a preliminary evaluation of the effect of suction distribution (prescribed or three-dimensional) on the vortex breakdown characteristics of strakes having the same general size and slenderness. Figure 12 presents a sample for one of the analytically designed strakes (AD 24) and for an empirically designed strake (ED 16) having the same area, along with their three-dimensional suction distributions. These two strakes have the same fixed R_a and R_b values but different shapes and R_s values. It is clear that the AD 24 gothic strake is the better of the two since it has the higher $\alpha_{BD\text{-}TE}$. This result might be unexpected since the ED 16 strake has a gothic shape

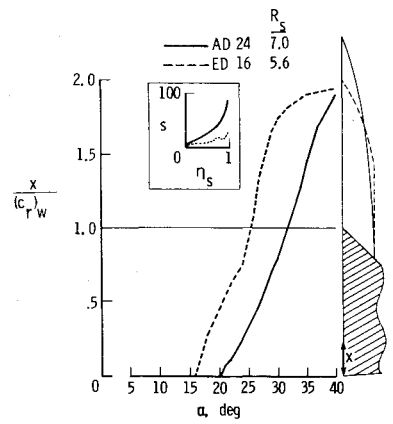

Fig. 12 Effect of strake geometry on breakdown and suction ($R_a = 0.325$).

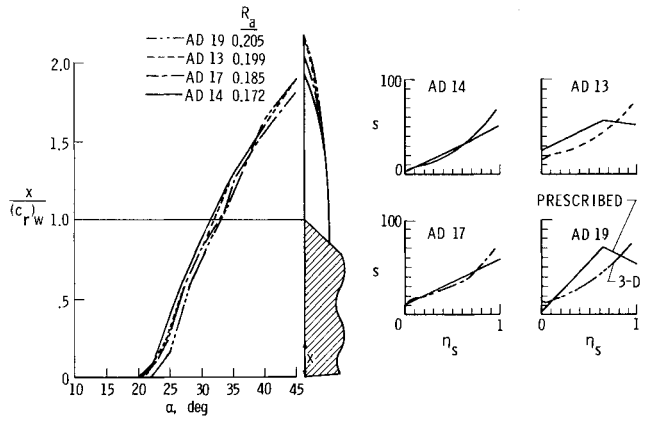

Fig. 13 Correlation of performance with suction.

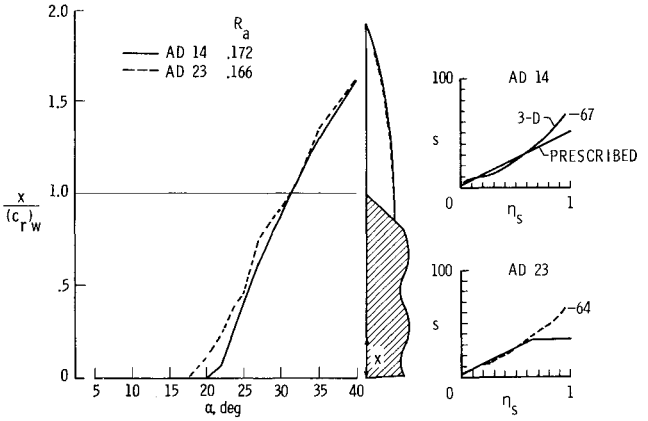

Fig. 14 Effect of small shape variation on breakdown and suction ($R_s = 7.0$, $R_b = 0.212$).

in the forward region followed by a substantial side edge. The side edge was added to stabilize the vortex and increase its strength, but this did not occur to the extent expected. Interestingly, this result is consistent for the two strakes in their s-η_s distributions, in that the tip value s_t and area of the AD 24 are higher than those of the ED 16. It is recognized, of course, that part of the decrease in performance from the AD 24 to the ED 16 is due to a reduction in R_s.

All of the preceding comparisons lead one to ask if strakes can be designed to have even higher $\alpha_{BD\text{-}TE}$ (i.e., better performance) and if so, can it be done with less area? This question is addressed in the next section.

Table 2 Correlation of performance with suction and area

Strake designation	$\alpha_{BD\text{-}TE}$, deg	s_t	R_a
AD 19	22	74	0.205
AD 13	21.5	73	0.199
AD 17	21	69	0.185
AD 14	20	67	0.172

Parameter Variations Leading to Improved Strakes

While the preceding discussions centered on the AD 24 strake, this section presents four different strake designs which realize comparable or better levels of performance than the AD 24 with about one-half to two-thirds its area. Their vortex breakdown characteristics and s-η_s distributions are presented in Fig. 13. Each of these strakes has an $\alpha_{BD\text{-}TE}$ that satisfies 20 deg $\leq \alpha_{BD\text{-}TE} \leq 22$ deg. As expected, the trend of increasing $\alpha_{BD\text{-}TE}$ is consistent with the increase in strake area. Although two of the accompanying prescribed s-η_s distributions are not specifically triangular, all four have high inboard slopes and reach high levels of suction near the tip. Furthermore, the three-dimensional s-η_s curves are very similar to one another, varying slightly in overall level and s_t value. Interestingly, even for the small 2 deg variation in $\alpha_{BD\text{-}TE}$ between the four strakes, the increase in s_t is in agreement with the increase in $\alpha_{BD\text{-}TE}$ and R_a. This can be seen more clearly by examining the three-dimensional s_t values in Table 2. Thus, s_t appears to be a useful feature in the design process.

One may possibly reason that the improved performance is a result of significant increases in area and slenderness ratio, these features being reflected only in the s-η_s distributions. Thus, it remains to be determined whether the vortex breakdown performance is sensitive to small perturbations in strake contour shaping. If it is, then are the changes reflected in the s-η_s distribution and, in particular, are they consistent with the design criterion described earlier?

In an attempt to shed light on these questions a comparison is made in Fig. 14 which illustrates the effect of small contour changes. This figure presents the vortex breakdown data and associated s-η_s distributions for two strakes, AD 14 and AD 23, which have the same R_s and R_b but a small variation in contour. The $\alpha_{BD\text{-}TE}$ for the two strakes differ by 2.5 deg although R_s and R_b are fixed and the areas differ by less than 4%.

The variation in contour between the two strakes is the result of the differences in the prescribed suction distributions used in the design procedure. It will be noted that the AD 14 prescribed suction distribution is more triangular than for the AD 23, which in turn leads to a shape that has a three-dimensional s-η_s which increases more rapidly and reaches a higher value at the tip. The experimental $\alpha_{BD\text{-}TE}$ results show that the AD 14 achieves a higher value than does the AD 23. Hence, this demonstrates that the vortex breakdown performance of a strake can be improved by making small refinements to its shape which lead to a higher value of s_t.

Conclusion

This paper has described a water-tunnel study of the vortex breakdown characteristics of a large number of analytically designed vortex strakes tested in combination with a moderate-aspect-ratio trapezoidal wing. The strake designs were based on a series of prescribed leading-edge suction distributions used in combination with a simplified flow, related to three-dimensional potential flow through certain simplifying assumptions. These prescribed suction

distributions considered the general observation made in an earlier study for delta wings in that increasing suction toward the tip provided improved vortex stability.

A wide range of strake sizes and slenderness ratios were covered, and this study presents a sample of that extensive parametric data base which may be of assistance in the preliminary phase of maneuvering aircraft strake design. Examples of the effects of the primary design parameters of size, span, and slenderness on the vortex breakdown characteristics were presented and analyzed in relation to the leading-edge suction distributions. Apart from these, there were several examples of detailed planform shaping on strakes of the same general size and slenderness. From these examples, it could be concluded that those strakes which, in general, simulated the design criterion in related flow produced three-dimensional leading-edge suction distributions which increased more rapidly near the tip to a higher value and led to a more stable vortex.

References

[1] Wentz, W.H. Jr., and Kohlman, D.L., "Wind Tunnel Investigations of Vortex Breakdown on Slender Sharp-Edged Wings," NASA CR-98737, 1968.

[2] Headley, J.W., "Analysis of Wind Tunnel Data Pertaining to High Angle-of-Attack Aerodynamics, Vol. 1: Technical Discussion and Analysis of Results," AFFDL-TR-78-94, July 1978.

[3] Smith, C.W., Ralston, J.N., and Mann, H.W., "Aerodynamic Characteristics of Forebody and Nose Strakes Based on F-16 Wind Tunnel Test Experience, Vol. 1: Summary and Analysis," NASA CR 3053, July 1979.

[4] Lamar, J.E., "Analysis and Design of Strake-Wing Configurations," *Journal of Aircraft*, Vol. 17, Jan. 1980, pp. 20-27.

[5] Frink, N.T. and Lamar, J.E., "Water Tunnel and Analytical Investigation of the Effect of Strake Design Variables on Strake Vortex-Breakdown Characteristics," NASA TP 1676, 1980.

[6] Lamar, J.E., and Gloss, B.B., "Subsonic Aerodynamic Characteristics of Interacting Lifting Surfaces with Separated Flow Around Sharp Edges Predicted by a Vortex-Lattice Method," NASA TN D-7921, Sept. 1975.